Available online at www.sciencedirect.com

ScienceDirect

Procedia Structural Integrity 17 (2019) 780–787

Structural Integrity Procedia

www.elsevier.com/locate/procedia

ICSI 2019 The 3rd International Conference on Structural Integrity

Numerical Simulations of Fatigue Crack Growth in a Steam Turbine Rotor Blade Groove

Jiří Kuželka[a], Martin Nesládek[a], Maxim Lutovinov[a], Josef Jurenka[a], Milan Růžička[a], Martin Rund[b], Petr Měšťánek[c]

[a]*Czech Tehnical University in Prague, Faculty of Mechanical Engineering, Technická 4, 16607 Praha 6, Czech Republic*
[b]*COMTES FHT a.s., Průmyslová 995, 33441 Dobřany, Czech Republic*
[c]*Doosan Škoda Power s.r.o., Tylova 1/57, 301 28 Plzeň, Czech Republic*

Abstract

With increasing share of renewable energy sources in the electricity production strict demands are placed on thermal power plants that have to cover the power shortages more frequently. Increasing number of steam turbine (ST) start-ups and shutdowns, as well as requirements on higher ramping of operating conditions, has detrimental effect on the overall lifetime of ST components. In the ST design process, this situation has to be dealt by applying advanced prediction methodologies handling the thermo-mechanical fatigue mechanism, for instance. On the other hand, in the case of currently operating STs, regular inspection and maintenance schedule as well as technologies for turbine operation control have to be reconsidered or newly developed. To cope with these challenges, the international consortium of energetic turbine producers and research institutes initiated the TURBO-REFLEX project funded by EU's H2020 program. One of the principal aims of the project is development of a damage tolerance approach that may be suitable for scheduling the ST rotor maintenance, for instance. Decisive factors in this effort are ST rotor operating conditions, material fracture properties and geometry that constitute the crack initiation site and crack growth rate and direction. This forms a complex task that has to be handled numerically by using a Finite Element (FE)-based code accompanied by in-house scripts for detecting the most probable way of crack propagation. In this contribution, the adopted fracture–mechanics approach applied to low-pressure section of ST rotor and results that have been achieved are presented.

Peer-review under responsibility of the ICSI 2019 organizers.

Keywords: fracture mechanics; fatigue crack growth; steam turbine;

1. Introduction

Even in virgin conditions not influenced by a previous loading history, structural materials often contain defects as microcracks or impurities that weaken the bulk material. On the other hand, in the case of hypothetical structurally

2452-3216
Peer-review under responsibility of the ICSI 2019 organizers.
10.1016/j.prostr.2019.08.104

homogeneous material, if a notched structure is made of it, cyclic stress concentration in the notch roots might initiate fatigue cracks. From the perspective of the material mechanical response, presence of these inhomogeneities manifests itself by altering the local stress-strain field considerably and to analyze it, numerical simulation tools are usually needed. Experimental and analytical investigation of the conditions that influence evolution of defects with respect to static or cyclic loading is the subject of the scientific discipline called fracture mechanics. Basically, it deals with assessing the crack stability and predicting the most probable crack growth direction and rate, i.e. the most important aspects that need to be answered if the residual lifetime of a structure containing defects is to be analyzed.

In recent years, several turbine rotor failures have been reported. The shutdown of this type of machine itself, at best, results in economic losses due to power supply cuts and necessary repairs. However, in case of a sudden brittle fracture, such event may result in catastrophic consequences including human losses. One of the well-known accidents of power generating turbines occurred in the German power plant Irsching in 1988 (Vrana et al., 2016). Because of the undetected flaw located near the center of low-pressure (LP) rotor forging, the shaft cracked and some parts broke through the turbine housing and were found up to 1.3 km far from the power plant. In this case, nobody was hurt, which unfortunately is not a case of turbine rotor failure reported in Nagasaki, 1970 (Nakao, n.d.). A microstructural flaw located in the shaft borehole caused brittle fracture of the entire rotor during performance tests of newly-installed turbine. The rotor fragments were thrown into the surroundings while killing 4 people. Stress corrosion cracking was the cause of brittle fracture of ST rotor installed in the Brittish nuclear power plant Hinkley Point after four years of commercial service (Nitta and Kobayashi, n.d.). The rotor fractured completely at five places while some of the parts flew out of the housing.

Less destructive ST rotor failures due to the stable crack growth will be most likely manifested by gradual increase in the rotor vibration intensity. Rotor vibrations are continuously monitored and emergency shutdown is initiated if they exceed limits. This scenario was followed in the rotor failure documented by Barella et al. (2011). In this case, a circumferential crack that initiated in a blade groove was observed. An interesting point is that the shaft residual cross sectional area was only about 25% of its original size. Most of the rotor failures are revealed by regular inspections and repaired by welding before a catastrophic scenario can occur (Mazur and Hernandez-Rossette, 2015).

One of the important parameters that should be considered in the ST rotor design and material selection is the so-called fracture appearance transition temperature (FATT, Rzepa, et al., 2017). To minimize probability of such catastrophic events due to the brittle fracture as mentioned above, the ST components' operating temperatures should be well above FATT. However, increasing demands on flexibility of STs that cause them to operate in unstable temperature conditions raise a question if this does not limit applicability of some materials in ST design.

The work presented in this paper is focused on numerical fatigue crack growth analysis (FCG) in an LP rotor section. More specifically, an initial flaw in the most stressed point of a rotor blade groove is assumed. Fracture-mechanics material parameters have been experimentally determined under the temperatures relative to FATT for the assumed CrMo rotor steel. In the linear FCG numerical simulation, the worst-case scenario of temperature 30 °C below FATT is assumed. The ABAQUS FE-code and in-house scripts have been employed for propagating the crack front. The paper clarifies the adopted approach and provides some preliminary results.

Crack growth analysis in steam turbine (ST) rotors is a challenging task due to the combination of mechanical and thermal loads. The induced material stress-strain response is a combination of start-stop cycles and superposed high-frequency loads that are mainly due to rotating mass and vibration of blades. As referred by Nesládek et al. (2018), depending on the turbine operating regime, thermo-mechanical load conditions may in the extreme case of cold-start regime induce small-scale yielding in high-pressure (HP) part of rotor. These conditions lead to alternating (tension-compression) stress time histories. Different situation may be observed in LP rotor sections, where the start-stop cycles induce linear elastic response, thus the repeated stress cycles with superposed high-frequency loads are found in this rotor domain.

In practical applications, the most used linear elastic fracture mechanics criterion to assess the crack stability is the so-called stress intensity factor (SIF) denoted as K_i, where $i = I, II$ or III depends on the bulk load mode (I is for tensile mode, II and III are for in-plane and out-of-plane shear modes, respectively). The SIF is defined as follows:

$$K_I = \lim_{r\to 0}\left[\sigma_{yy}(2\pi r)^{\frac{1}{2}}\right] \to \sigma\sqrt{\pi a}\cdot Y(a,W,L,\dots),$$
$$K_{II} = \lim_{r\to 0}\left[\tau_{xy}(2\pi r)^{\frac{1}{2}}\right] \to \tau\sqrt{\pi a}\cdot Y(a,W,L,\dots), \quad (1)$$
$$K_{III} = \lim_{r\to 0}\left[\tau_{yz}(2\pi r)^{\frac{1}{2}}\right] \to \tau\sqrt{\pi a}\cdot Y(a,W,L,\dots),$$

where σ_{yy}, τ_{xy} and τ_{yz} are tensile and shear stress tensor components in Cartesian system with origin in the crack tip, xy-plane normal to the crack surface and z-axis tangent to the crack front. σ and τ are normal and shear in-plane or out-of-plane nominal stresses, dimensionless factor $Y()$ represents an influence of geometry and load conditions.

Another important aspect that has to be dealt with in the crack analysis is prediction of the crack growth direction. The Maximum Tangential Stress (MTS) criterion (Erdogan and Sih, 1963) postulates that the crack front propagates in the direction perpendicular to the maximum tangential stress - see the stress tensor components expressed in polar coordinate system as shown in Fig. 1.

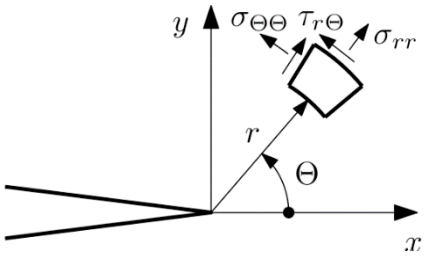

Fig. 1. Stress tensor components in polar coordinate system at the crack front.

Prediction of FCG rate usually relies on measurement of FCG curves for the purpose of finding the relation $v = v(\Delta K)$. Asymptotic values denoted as ΔK_{th} and ΔK_c stand for threshold SIF range and the critical SIF range. ΔK_{th} represents the minimum SIF range that a crack front has to be subjected to for propagation. On the other hand, ΔK_c is the limit SIF range leading to ultimate rupture.

The region of stable crack propagation usually conforms well to the so-called Paris law (Paris and Erdogan 1963):

$$v = \frac{da}{dN} = C\Delta K_{eff}^{m}, \quad (2)$$

where C and m are regression coefficients and ΔK_{eff} is the effective SIF range defined as

$$\Delta K_{eff} = K_{max} - K_{op}. \quad (3)$$

K_{max} is the SIF at the peak stress, whereas K_{op} is the minimum SIF that opens the crack.

Mean stress effect is often less pronounced in the Paris region and may be well handled by employing ΔK_{eff}. Several formulas correlating ΔK_{th} to the R ratio may be found in the literature. Klesnil and Lukáš (1972) published the following formula

$$\Delta K_{th} = (1-R)^{\gamma}\Delta K_{tho}, \quad (4)$$

where γ is a material constant and ΔK_{tho} is the SIF range for $R = 0$. From a practical point of view, the most usable relationship seems to be the one published by Kujawski and Ellyin (1995):

$$\Delta K_{th} = \Delta K_{tho}\frac{1.8}{\left\{\frac{1+R}{1-R} + \left[\left(\frac{1+R}{1-R}\right)^2 + 4\right]^{\frac{1}{2}}\right\}^{\frac{1}{2}}}, \quad (5)$$

where no material constant is used.

2. Experimental work

For the examined CrMo steel applicable to LP rotor section, Charpy impact tests to determine FATT have been carried out. The adopted test procedure was in accordance with ASTM E 23 standard, considering FATT as a temperature at which 1:1 ratio of brittle and ductile fracture may be observed on fracture surfaces.

Two sets of material samples have been extracted from semi-finished rotor disk, the first one from the disk circumferential surface and the other from the disk center, in order to find out the differences if they exist. Fig. 2 shows percentage share of brittle fracture depending on temperature. Refer to Rzepa et al. (2017) for more details on the adopted procedure for evaluating the share of brittle fracture from the specimen fracture surface morphology. By regression analysis of the experimental data, FATT may be directly obtained as illustrated in Fig. 2. For the two sets of material samples, the FATT is almost identical and roughly equal to 30 °C.

Experimental campaign to determine ΔK_{th}, Paris law and K_{Ic} for temperatures relative to the FATT has been initiated. Elevated and reduced temperature conditions were ensured by testing in temperature chamber. Measurement of ΔK_{th} and FCG rates in the Paris region have been conducted separately. Fig. 3 shows the experimental setup employed for these tests. Electro-magnetic resonance fatigue testing machine RUMUL was used to drive the specimen force-controlled loading in cycles with $R = 0.1$ and 100 Hz frequency. Single-specimen tests repeated on 3-4 samples were carried out. CT specimens were designed according to recommendations in ASTM E 647 standard – Fig. 4(a). Fatigue crack length was detected by the direct current potential drop technique (DCPD) and ΔK values were determined by analytical procedure according to the ASTM E 647 standard. After unloading, the specimens were annealed to mark the cracks, cooled in nitrogen and broken in order to verify accuracy of the crack length measurements. Sample measurement outputs corresponding to temperature FATT – 30 °C are shown in Fig. 5.

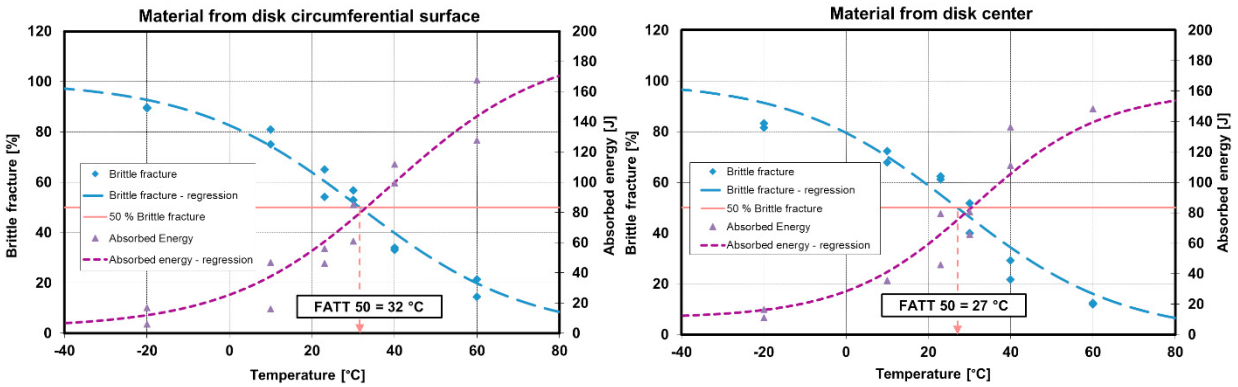

Fig. 2. Results of Charpy impact tests and evaluation of FATT.

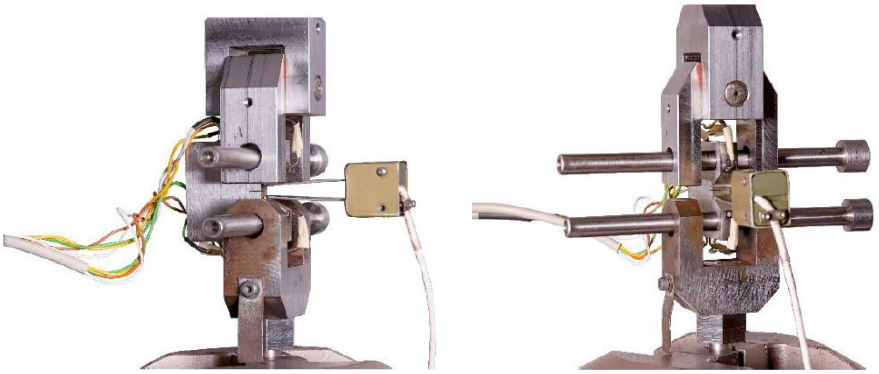

Fig. 3. Experimental setup for FCG and ΔK_{th} measurements.

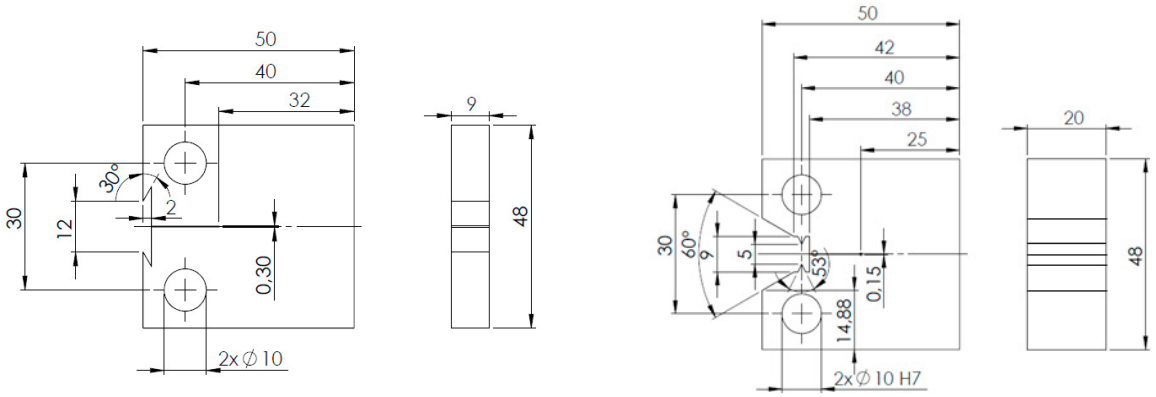

Fig. 4. Geometry of test samples for FCG and ΔK_{th} (a) and K_{Ic} (b) measurements.

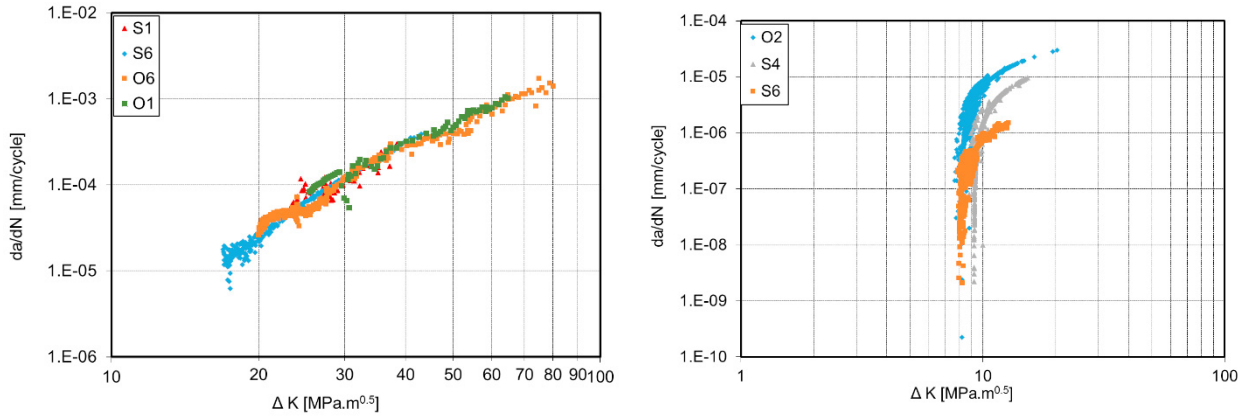

Fig. 5. Sample outputs of FCG and ΔK_{th} measurements.

Tab. 1. K_{Ic} values obtained under various temperatures.

	Temperature		
	FATT - 30 °C	FATT	FATT + 30 °C
K_{Ic} $[MPa \cdot m^{0.5}]$	94.2 ± 8.9	129.2 ± 25.9	262.0 ± 90.6

Fracture toughness K_{Ic} was identified by the experimental procedure according to the ASTM E399. Quasistatic monotonic loading was applied to specimens designed according to Fig. 4(b). Crack mouth displacement was measured by clip-on extensometer. Values of the obtained K_{Ic} for the considered temperatures are in Tab. 1. As indicated by the standard deviations, data is affected by high scattering, which is due to the material sensitivity on deviations in test temperatures close to FATT.

3. FCG simulations

A fir-tree blade groove from an LP rotor section of a ST was the subject of FCG numerical simulations. Linear elastic material response is assumed with ΔK as a decisive parameter in crack stability and FCG rates assessment. The MTS

criterion was used to detect the most probable direction of 3D crack propagation. The material mechanical response is due to the rotor and blade centrifugal forces (start-stop cycles) and superposed high-frequency loads manifested as blade bending.

A set of in-house scripts for FCG simulation was developed. The adopted procedure of FCG simulation is illustrated in Fig. 6(a). In this calculation, an initial edge flaw is assumed to be present in the locality subjected to the maximum 1st principal stress. FE-based commercial software ABAQUS is used for crack surface generation in LP rotor geometry, re-meshing and stress-strain response analysis in any actual increment of crack propagation. The crack shape is defined by array of points coordinates forming crack fronts. The last item in array corresponds to actual crack front, the rest to previous crack fronts. A spline interpolation through crack front points is used to form a smooth crack front. A linear interpolation between the consecutive crack fronts is used to form free crack surfaces defined as the seam entity in ABAQUS.

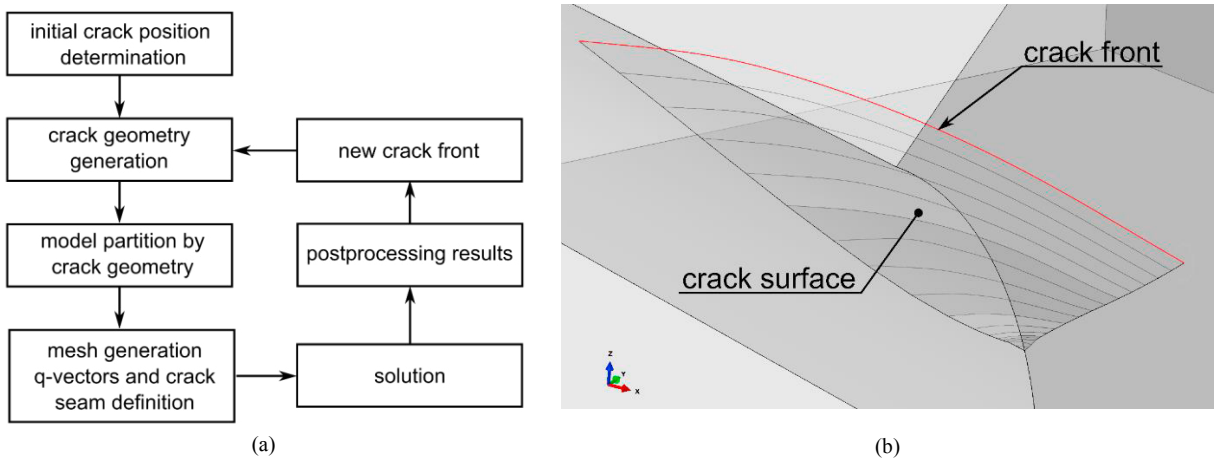

Fig. 6. Flow chart of FCG simulation (a), visualization of free crack surfaces modeled by the adopted procedure (b).

Thus the crack is defined as a geometric entity in the model as can be seen in Fig. 6(b). A sequence of geometry operations is applied to create a proper geometry around crack tip needed for high-quality mesh. A coordinate system with origin at each node on the crack front is defined having orientation in the direction of crack face normal and MTS-predicted course of crack propagation.

The SIF amplitudes and crack propagation directions along crack front are extracted from the ABAQUS result files. Values in the outmost nodes are excluded due to their inaccuracy and the rest is smoothed by Savitsky - Golay filter to avoid fluctuations in the resulting crack front shape. The crack length increments along crack front and corresponding cycles are computed according to Paris law (2), which was calibrated by the FCG experiments presented in the chapter 2. The minimum crack length increment is selected and the rest of increments along crack front is computed as proportional to SIF amplitudes. The increments are finally smoothed to avoid the oscillations in crack front shape caused by stress redistributions. When the increment along crack front is known, new crack front can be set and whole process can be repeated.

4. Results and discussion

Sample SIF amplitude and corresponding crack length increment can be seen in Fig. 7. The solid line in Fig. 7(a) represents filtered and smoothed ΔK due to start-stop cycles, while the red dots are the original nodal data retrieved from the ABAQUS result files. This sample result justifies the need for censoring the data at the outmost nodes of the ABAQUS model. The zero value of the normalised position in the plots means location at the blade groove fillet surface. The obtained FCG rates in the groove axial direction are more than two times greater than in the rotor tangential direction (position 1.0 in the plots) as may be deduced here from the plot in Fig. 7(b).

FCG curve determined numerically is shown in Fig. 8(a). The crack length is measured in the groove axial direction. Since the initial flaw was placed at the location of the maximum 1st principal stress, a drop in the FCG rate may be observed once it reaches approximately 15 mm length as a consequence of lower stress.

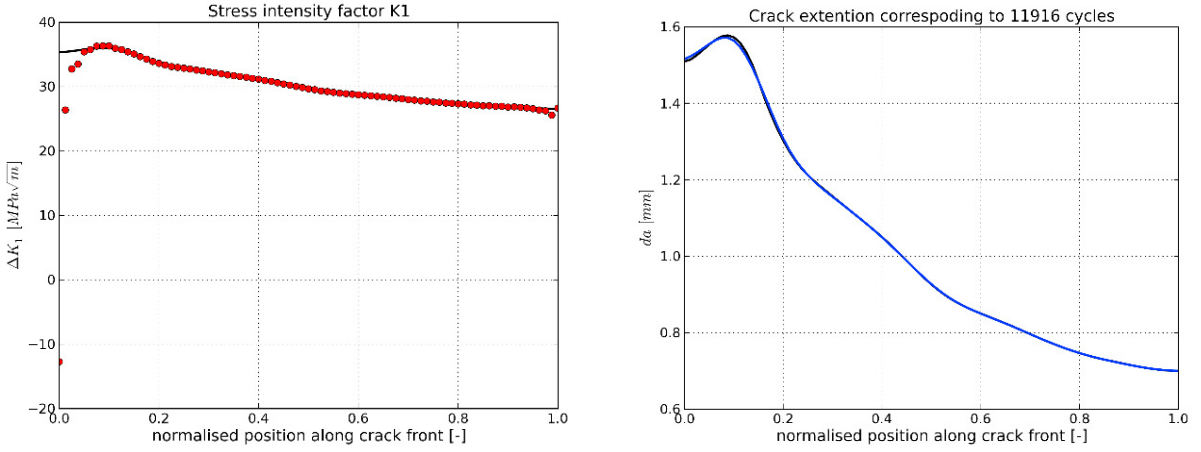

(a) (b)

Fig. 7. Computed SIF amplitude (a) and corresponding crack increment (b) along crack front.

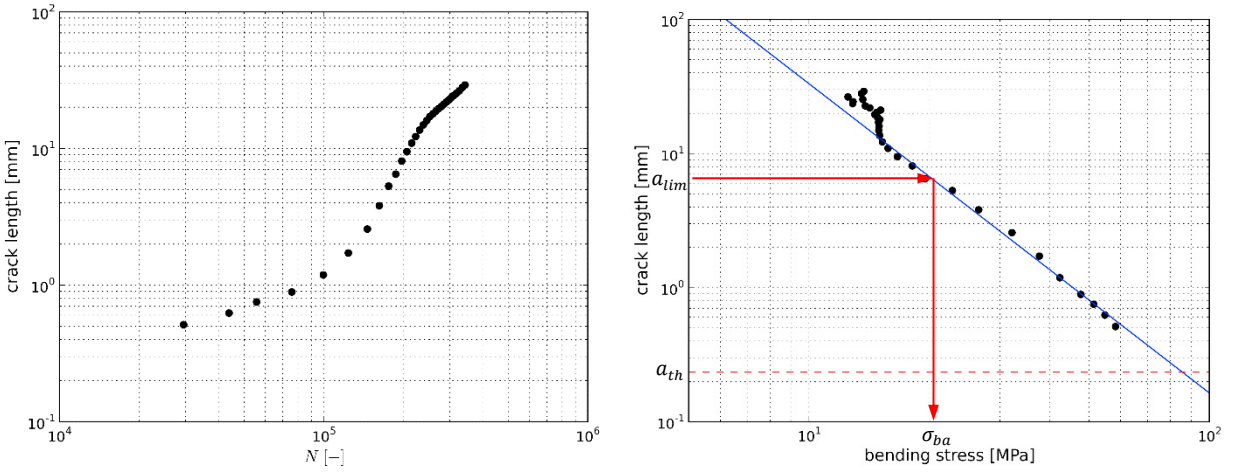

(a) (b)

Fig. 8. FCG curve determined by the numerical procedure (a), the diagram showing the dependence of the threshold bending stress on the crack length (b).

The diagram in Fig. 8(b) is a graphical representation of the dependence of the threshold bending stress on the crack length. These data were obtained by propagating the crack to a specific length (plotted on the vertical axis) due to the start-stop cycles followed by unit bending load representing blade vibration. Knowing the experimentally determined ΔK_{th}, the threshold bending stress may be determined subsequently. It is plotted on the horizontal axis and expressed as a nominal bending stress amplitude acting on the blade root cross-section normal to radial. Using this diagram, the minimum bending stress amplitude σ_{ba} that propagates the crack may be easily determined for a certain crack length a_{lim}. Note that the a_{th} value is the threshold crack length propagated by the start-stop cycles, which is equal to 0.25 mm in this case.

It was found that the crack tends to propagate from the groove fillet to the blade root-groove contact zone long before it reaches the critical SIF range ΔK_{Ic}. To simulate this properly and to determine the critical crack length, the FE model should be improved by involving more realistic friction contact conditions in the simulation.

The assumed temperature for FCG simulations was FATT – 30 °C, which is 0 °C for this batch of material and is well below the LP rotor operating conditions. However, according to the experience with the material being investigated, the FATT value differs in the individual batches and may be close to the conditions during the start of the turbine before reaching the stabilized temperature. This justifies the decision to choose the material properties applicable to such a low temperature.

5. Conclusions

The paper is a brief introduction to the fracture-mechanics approach applied to FCG simulations in a LP rotor section of a ST. Experimental investigation of the Paris law, ΔK_{th} and K_{Ic} has been performed and sample results are presented in this text. Based on these experimental data, numerical simulations of FCG based on ABAQUS and in-house codes could be carried out. FCG curve of a crack initiated from the location subjected to the maximum 1st principal stress was numerically identified. It was found that FCG rates in the rotor blade groove axial direction are more than two times greater than in the rotor tangential direction. The diagram that correlates the crack length due to the turbine start-stop cycles to the threshold nominal bending stress due to blade vibrations was constructed.

Acknowledgements

This project has received funding from the European Union's Horizon 2020 research and innovation program under the Grant Agreement 764545 – TURBO-REFLEX.

References

Barella, S., Bellogini, M., Boniardi, M., Cincera, S., 2011. Failure Analysis of a Steam Turbine Rotor. Engineering Failure Analysis, 18, pp. 1511-1519.

Erdogan, F., Sih, G.C., 1963. On the Crack Extension in Plates Under Plane Loading and Transverse Shear. Journal of Basic Engineering, 85(4), pp. 519-525.

Klesnil, M., Lukáš, P., 1972. The Effect of Stress Cycle Asymmetry on Fatigue Crack Growth. Materials Science and Engineering, 9, pp. 231-239.

Kujawski, D., Ellyin, F., 1995. A Unified Approach to Mean Stress Effect on Fatigue Threshold Conditions, International Journal of Fatigue, 17(2), pp. 101-106.

Mazur, Z., Hernandez-Rossette, A., 2015. Steam Turbine Rotor Discs Failure Evaluation and Repair Process Implementation. Engineering Failure Analysis 56, pp. 545-554.

Nakao, M., n.d. Brittle Fracture of Turbine Rotor in Nagasaki. JST Failure Knowledge Database. Available online: http://www.sozogaku.com/fkd/en/hfen/HA1000601.pdf. Accessed 30 May 2019.

Nesládek, M., Jurenka, J., Bartošák, M., Růžička, M., Lutovinov, M., Papuga, J., Procházka, R., Džugan, J., Měšťánek, P., 2018. Thermo-Mechanical Fatigue Analysis of a Steam Turbine Shaft. Acta Polytechnica CTU Proceedings, 20, pp. 56-64.

Nitta, A., Kobayashi, H., n.d. Burst of Steam Turbine Rotor in Nuclear Power Plant. JST Failure Knowledge Database. Available online: http://www.sozogaku.com/fkd/en/hfen/HB1031029.pdf. Accessed 30 May 2019.

Paris, P.C., Erdogan, F., 1963. A Critical Analysis of Crack Propagation Laws. Journal of Basic Engineering, 85(4), pp. 528-534.

Rzepa, S., Bucki, T., Konopík, P., Džugan, J., Rund, M., Procházka, R., 2017. Influence of Specimen Dimensions on Ductile-to-Brittle Transition Temperature in Charpy Impact Test, IOP Conference Series: Materials Science and Engineering, 179.

Vrana, J., Zimmer, A., Lohmann, H.-P., Heinrich, W., 2016. Evolution fo the Ultrasonic Inspection over the Past Decades on the Example of Heavy Rotor Forgings. 19th World Conf. on Non-Destructive Testing.